Journal of Nepal Geological Society, 2023, Vol. 65 (Sp. Issue), pp. 99–106
https://doi.org/10.3126/jngs.v65i01.57769

Earthquake impact on the stress magnitude at the area of shear zones

Krishna Kanta Panthi[1,*] and Chhatra Bahadur Basnet[2]

[1]Department of Geoscience and Petroleum, Norwegian University of Science and Technology (NTNU), S. P. Andersen Vei 15a 1, 7491 Trondheim, Norway
[2]Clean Energy Consultants Pvt. Ltd., Kathmandu, Nepal
**Corresponding author's email: krishna.panthi@ntnu.no*

ABSTRACT

Both tectonic activity and geological environment such as faulting and shearing in the rock mass influences the in-situ stress condition in the rock mass. The large-scale earthquakes cause both accumulation and sudden release of strain energy resulting the changes on the magnitude and direction of the in-situ stresses. This is the case in the Himalayan region, where the tectonic movement is active and periodic dynamic earthquakes are common. This manuscript assesses the influence of local shear faults on the in-situ stress condition along the pressure tunnel of Upper Tamakoshi Hydroelectric Project in Nepal. For this a 3D numerical modeling is carried out to assess potential changes in the magnitude of in-situ stresses, in particular the magnitude of minimum principal stress, due to dynamic loading (earthquake).

Keywords: Pressure tunnel, in-situ stresses, 3D numerical modelling, Himalayan geology, earthquake

Received: 27 February 2023 **Accepted:** 08 June 2023

INTRODUCTION

Sufficient minimum principal stress is required to avoid hydraulic jacking along the shotcrete lined/unlined pressure tunnels. A systematic and step wise evaluation of the in-situ stress condition is a key factor for the successful design of shotcrete lined/unlined pressure tunnels in the Himalayan region where frequent earthquakes are very common (Panthi and Basnet, 2019). At the Upper Tamakoshi Hydroelectric Project (UTHEP), the in-situ stresses were initially measured by SINTEF (2008) using 3D over-coring at the test excavated tunnel located on the bank of Tamakoshi River near Gongar. The location of powerhouse cavern, vertical penstock shaft and headrace tunnel were fixed based on the measured in-situ stresses in 2008. In the design, a decision was made to introduce a shotcrete lined high pressure headrace tunnel with a maximum hydrostatic pressure of about 42 Bars (420 m hydrostatic head) following vertical penstock shaft. However, the minimum principal stress measured by hydraulic fracturing (SINTEF, 2013) at the end of the pressurized headrace tunnel showed insufficient minimum principal stress. This forced the designer to make a design change with an introduction of new vertical penstock shaft so that potential hydraulic jacking and leakage through the headrace tunnel is avoided (Panthi and Basnet, 2017). According to McGarr and Gay (1978) and Panthi (2012, 2014), the in-situ stress field at a particular region is influenced by geological and geo-tectonic history and topography. The Himalayan region is tectonically active where medium to large scale earthquakes occur periodically. A dynamic stress analysis is pre-condition for the assessment of the magnitude of minimum principal stress which provides basis for the design of shotcrerte lined pressure tunnels (Panthi and Basnet, 2019).

The aim of this manuscript is to evaluate the in-situ stress state of UTHEP area with due consideration of both static and dynamic (earthquake) loading conditions. A 3D numerical model was used for the assessments since it gave possibility to incorporate complex topography and geological structures like weakness and shear zones. First, field measured in-situ principal stresses were used to validate the model under static condition. Then, the earthquake aftershocks (Mw 7.3) of 12th May 2015 which had an epicenter nearby the project area after a major Gorkha earthquake (Mw 7.8) of 25th April 2015 was considered in the dynamic analysis. Peak ground accelerations (PGA) of the aftershock at the project area generated by USGS (2015) were used to validate the model for dynamic analysis. The difference between the magnitudes of minimum principal stresses from these two analyses at different locations along the headrace tunnel alignment were evaluated to assess permanent changes in the magnitude of minimum principal stresses.

UPPER TAMAKOSHI HYDROELECTRIC PROJECT

The UTHEP, construction completed in 2021, has an installed capacity of 456 MW. The project exploits 66 m^3/sec design discharge and 822 m gross head to generate the energy (Panthi and Basnet, 2017). The project consists of civil structures like headworks, headrace tunnel, vertical penstock shafts, and underground powerhouse cavern, tailrace tunnel and access tunnel (Fig. 1).

At the UTHEP headrace system, there were several changes made during the design and construction stages of the project. In 2008, the headrace tunnel was designed to have a maximum static water head of about 420 m (4.2 MPa), which is explained as 'OLD HRT' in this manuscript. After the measurement of minimum principal stress at the downstream end of high-pressure headrace tunnel, it was realized that the rock mass is not capable to sustain 420 m hydrostatic head by a shotcrete lined headrace tunnel. This condition led to the change in the headrace tunnel alignment more at an upper level as indicated in Figure 2. The maximum static water head in this new

alignment is now limited to about 115 m (1.15 MPa), which is denoted as 'NEW HRT' in this manuscript.

It is emphasized here that the magnitudes of minimum principal stresses along the alignment were the matter of major concern for the implementation of shotcrete lined pressurized headrace tunnel. The topographic condition prevailing, presence of major weakness and shear zones, recent major earthquake activities surrounding the project area are the main issues that have direct effect on the magnitude and orientation of the in-situ stresses.

Geo-tectonics

Geologically, the project is in the Higher Himalayan Tectonic Formation of eastern Nepal Himalaya (Fig. 1) where Precambrian high grade metamorphic rocks such as gneiss, quartzite, marbles, migmatite and granitic gneiss are found (Norconsult and Lahmeyer, 2008). Main rock types at the project area are micaceous schist and banded gneiss with considerable amount of mica content (Basnet and Panthi, 2021). Rock mass in the project area consists of foliation joints and two sets of cross joints. The general strikes of the foliation joints are WSW to WNW with dip angles of 35–75° NW to NE.

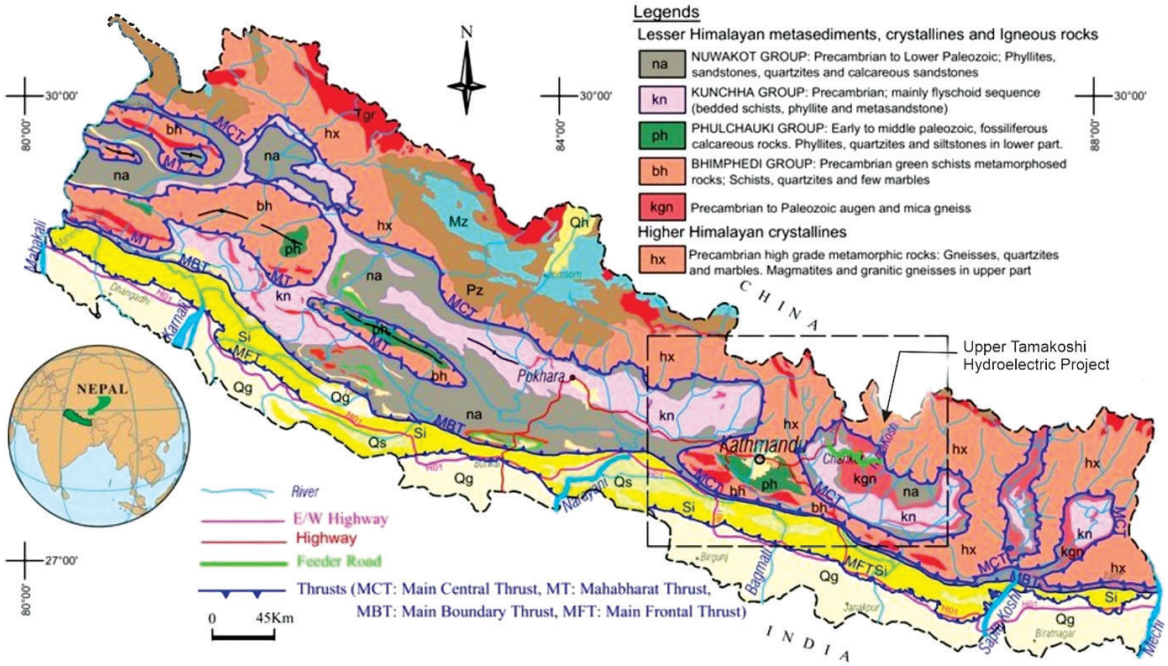

Fig. 1: Location of UTHEP in the geological map of Nepal.

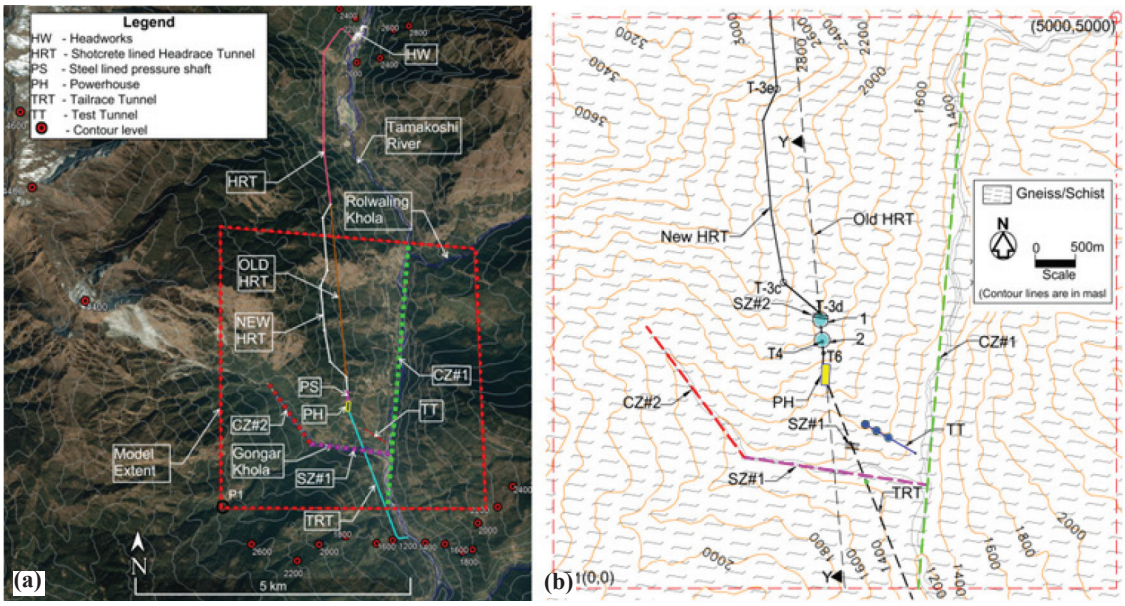

Fig. 2: (a) 3D topography with major lineaments and layout of UTHEP overlaid in Google Earth map, (b) topographic map of the project area inside selected model extent (Panthi and Basnet, 2019).

As shown in Figure 2a, the headrace tunnel is oriented along the right bank of the Tamakoshi River. The highest elevation of the nearest hill from the headrace tunnel is about 4500 masl and the lowest elevation is at the Tamakoshi River at about 1250 masl. The elevation difference is hence about 3300 m within a horizontal distance of about 5500 m where slope of the terrain varies from 30 to 40° indicating that the Tamakoshi River has a deep valley, and the topography represents a high relief. The Gongar Khola (a small river) near the outer reach of the headrace tunnel makes another deep valley which has an elevation of about 1250 masl at the confluence with Tamakoshi River. The Tamakoshi River is represented as a crushed zone CZ#1 and the upper left tributary of the Gongar valley is represented as a crushed zone CZ#2. In addition, four more weakness zones were encountered during tunnel excavation which are represented as shear zones SZ#1, SZ#2, SZ#3 and SZ#4 (Figs. 2b, 3a,b).

The orientations of these shear zones follow the orientation of the foliation joints in the rock mass. Figure 3a shows the old headrace tunnel alignment (OLD HRT) and the changed headrace tunnel alignment during construction (NEW HRT).

In-situ stresses

Both 3D-overcoring and hydraulic fracturing techniques were used to measure the in-situ stress state at different locations (Fig. 4). The measurements were carried out at two different elevation levels of the topography at different project development stages.

The in-situ stresses were measured at locations TT1, TT2 and TT3 in test tunnel (TT) located at the valley level of Gongar and Tamakoshi valleys in 2008 by 3D-overcoring technique (SINTEF, 2008). The mean values of principal stresses with respective standard deviations and orientation of corresponding stresses are given in the Table 1. The stress information were used during detail design as a basis for the location design of the shotcrete lined headrace system as indicated "OLD HRT" in Figure 3a.

However, after about 265 m excavation of the OLD HRT from the downstream end, a shear zone SZ#2 was encountered (Fig. 3). After headrace tunnel excavation of about 200 m (up to point EE in Fig. 3a), it was understood that the rock mass at the downstream end of the headrace tunnel is de-stressed.

Hence, following the recommendations made during detailed design, hydraulic fracturing test was carried out to ascertain suitability of the shotcrete lined pressure tunnel with 420-meter static head (4.2 MPa). The magnitude of minimum principal stress was measured by SINTEF (2013) at locations 1 and 2 along the excavated tunnel (Fig. 4). Altogether, 7 measurements at different depths of four boreholes at location 1 and 19 measurements at different depths of four boreholes at location 2 were made. Table 2 gives the summary results of the evaluation of minimum principal stress (S_3), tensile strength (S_t) and maximum principal stress (S_1) for both locations 1 and 2. As seen in Table 2, the measured minimum principal stress at location 1 is lower than the static water head pressure of 4.2 MPa indicating hydraulic fracturing.

The 2015 Earthquake

An earthquake with a magnitude of Mw 7.8 occurred on 25th of April 2015 with an epicenter at Barpak village which is famously known as the Gorkha Earthquake 2015. Series of aftershocks of varying magnitudes occurred following this main event. Figure 5 is a plot of numerous aftershocks of varying magnitudes (more than Mw 4) that have been registered for the period from 25th of April 2015 to 2018.

As shown in Figure 5, the strongest aftershock with magnitude of Mw 7.3 occurred at NE-Kalinchowk at Dolakha district on 12th May 2015. The UTHEP is within 13 km proximity from the epicenter of this aftershock. The seismic waves generated during the aftershock of Mw 7.3 are the most influential regarding in-situ stress changes in the project area (Panthi and Basnet, 2019).

STRESS STATE ANALYSIS

Tectonic, gravitational stresses and geological defects such as weakness and fault zones which locally influence on the in-situ stress state by perturbing the stress trajectories are important inputs in numerical analysis. Hence, the numerical modelling using FLAC^{3D} (ITASCA, 2017) was used at UTHP

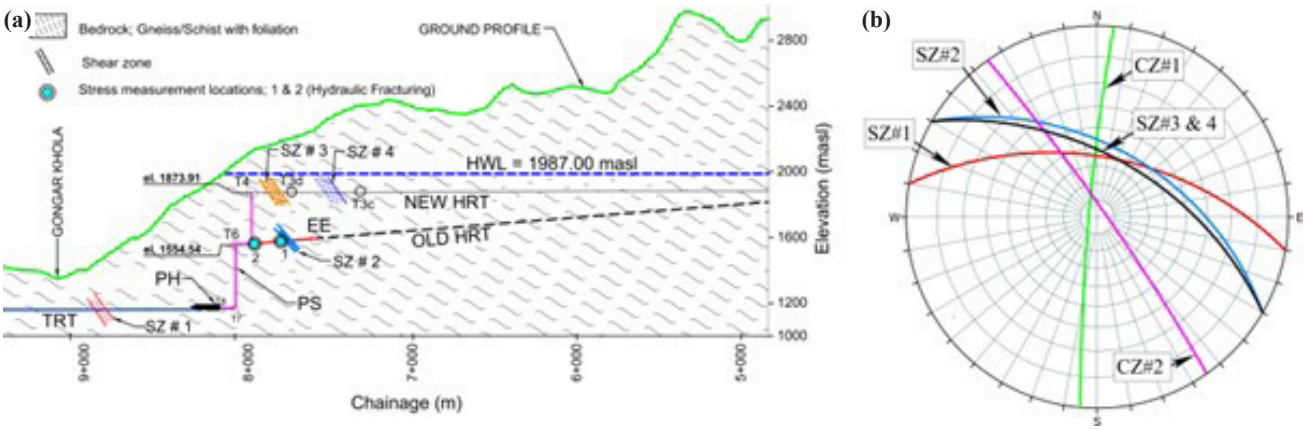

Fig. 3: (a) Tunnel alignment profile with geology ('HWL' is head water level), (b) stereographic projection of weakness zones (Panthi and Basnet, 2019)

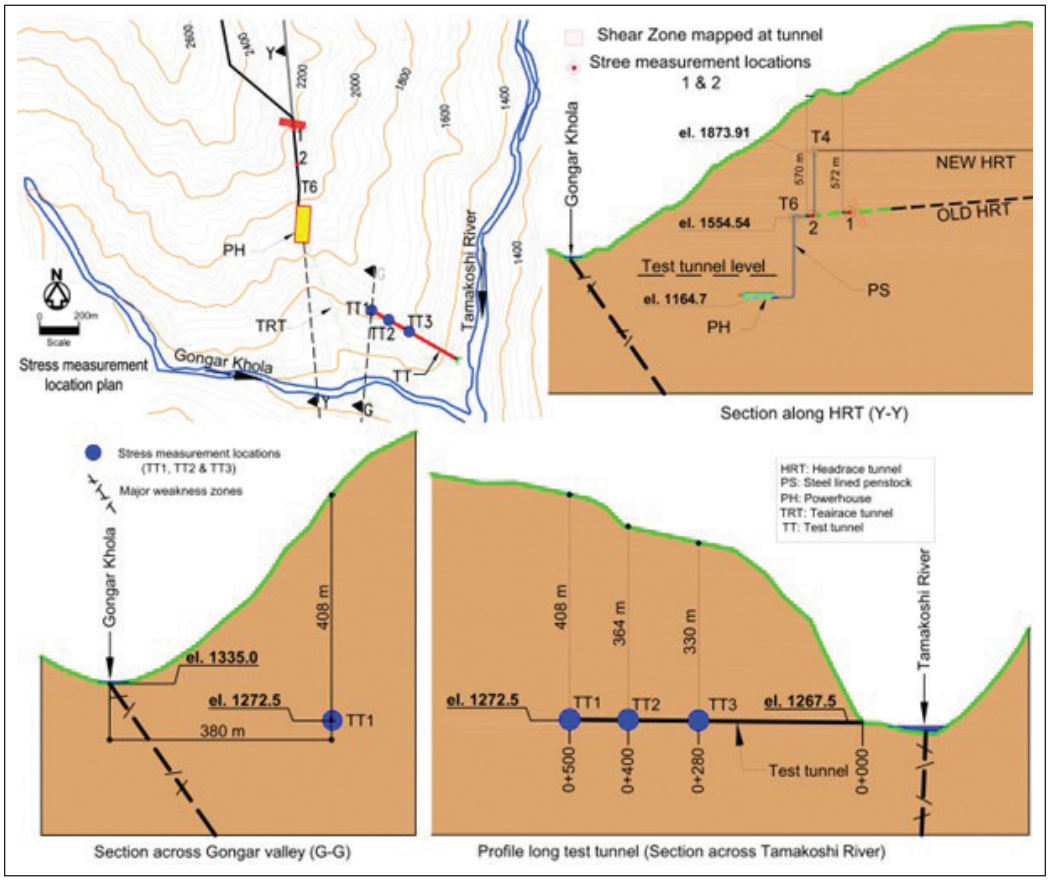

Fig. 4: Stress measurement locations TT1, TT2, TT3, 1 and 2 (Panthi and Basnet, 2019).

Table 1: Final magnitude and orientation of principal stresses at TT1, TT2 and TT3.

Principal stresses	TT1			TT2			TT3		
	MPa		Orientation	MPa		Orientation	MPa		Orientation
	Mean	Sd		Mean	Sd		Mean	Sd	
Maximum, S_1	18.4	2.9	120/28	17.4	2.2	205/30	21.6	3.8	021/10
Intermediate, S_2	12.4	4.7	240/42	10.8	1.7	100/23	12.6	2.8	117/27
Minimum, S_3	7.1	1.8	009/35	1.1	2.7	339/50	6.4	4.8	272/61

Table 2: Stress measurement by hydraulic fracturing at locations 1 and 2.

Location	S_3 (MPa)		S_t (MPa)		S_1 (MPa)	
	Mean	Sd	Mean	Sd	Mean	Sd
1	3.2	1.0	10.0	1.2	10.1	3.2
2	5.4	2.5	10.0	1.2	14.2	6.0

to quantify the stress magnitudes at the locations of interest. Both static and dynamic analyses were carried out. In static analysis, the measured stresses were used to validate the model and minimum principal stresses were identified at the tunnel locations. The statically validated model was further exploited for the dynamic loading to assess seismic influence on the stress state.

FLAC^{3D} model

The modelling strategy was adopted following Stephansson and Zang (2012) as indicated in Figure 6. The rock mechanical parameters were assigned in the model considering rock mass as isotropic and linearly elastic material. The interfaces representing the major weakness and shear zones (CZ#1, CZ#2, SZ#1, SZ#2, SZ#3 and SZ#4) were introduced with interface parameters (Fig. 7).

Both static and dynamic analyses were carried out using FLAC^{3D} software (ITASCA, 2017). Geometry, material properties, boundary and initial conditions were defined for the model extent generated in FLAC^{3D} model. The Tamakoshi project area has a higher Himalayan Crystalline rock formation consisting of schistose gneisses. The homogeneity in the rock mass is disturbed by major and minor shear and weakness zones (largescale discontinuities) as indicated in the model (Fig. 7). The rock mass was considered as isotropic material even though the gneiss has some degree of anisotropic behavior due to schistosity. The constitutive equations derived for a linearly elastic model was used where the material is expected to exhibit linear stress-strain behavior. Principally the adopted

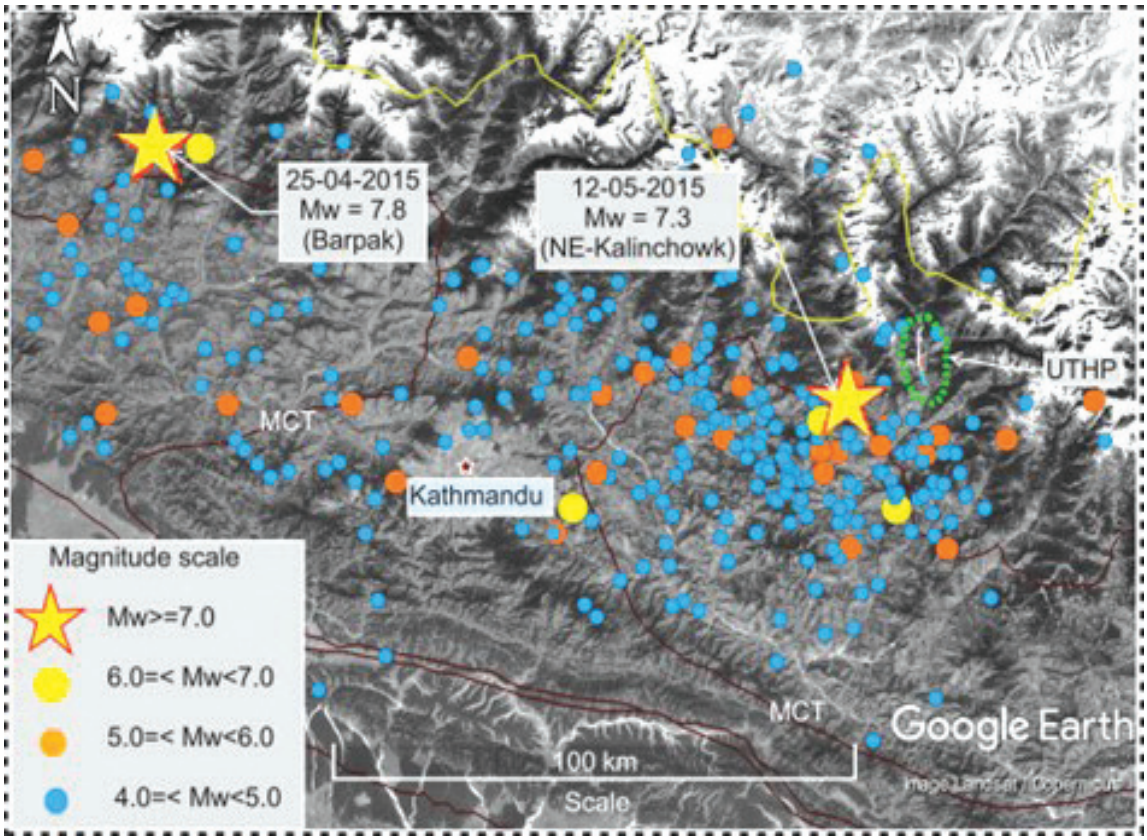

Fig. 5: Recorded earthquakes in and around the Upper Tamakoshi project area (inside the rectangle shown in Figure 1) after the Gorkha Earthquake of April 2015. Note: The earthquake data were taken from U.S. Geological Survey and overlaid in Google Earth map; Mw is moment magnitude.

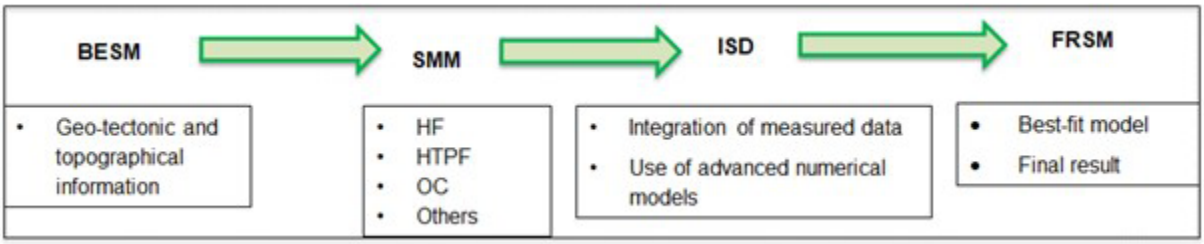

Fig. 6: Flowchart showing steps of in-situ stress assessment approach used in the analysis.

approach is correct for the in-situ stress state evaluation of a large area as of UTHEP and therefore the assumptions are representative enough to find the in-situ stress state at UTHEP.

The magnitude and orientation of the maximum tectonic stress (S_{Tmax}) and the minimum tectonic stress (S_{Tmin}) were assumed with an orientation of the maximum tectonic stress as θ. The total horizontal stress towards the tectonic stress directions for each zone was then calculated by adding gravity led horizontal stress and the initially assumed tectonic stress magnitudes. The total horizontal stresses were resolved towards both X- and Y-axes as normal stresses (S_{xx} and S_{yy} respectively) and in XY-plane as shear stresses (S_{xy}). The total normal and shear stresses were further initialized in each zone for whole geometry and the model was run for the equilibrium state once again. The process was repeated multiple times for various combinations of tectonic stress magnitudes and orientations until the simulated principal stresses converge to corresponding principal stress magnitudes measured at the test tunnel (Table 1). The output of the validated model represents as 'Static Analysis'.

After the static analysis, a seismic acceleration was applied at the base of the model as a dynamic loading. The seismic acceleration is applied in three mutually perpendicular directions, i.e., along North-South, East-West and Vertical directions. The model was run for the specified dynamic time-period. The acceleration at a specified crest point was tracked during the simulation and the peak values were evaluated. The peak values of the acceleration were compared with the PGA at the same point. The amplitude of base acceleration was changed until the simulated peak acceleration at the surface becomes sufficiently close to the PGA at the same surface location. Once the simulated value was found close enough to the PGA, the model was said to be dynamically validated.

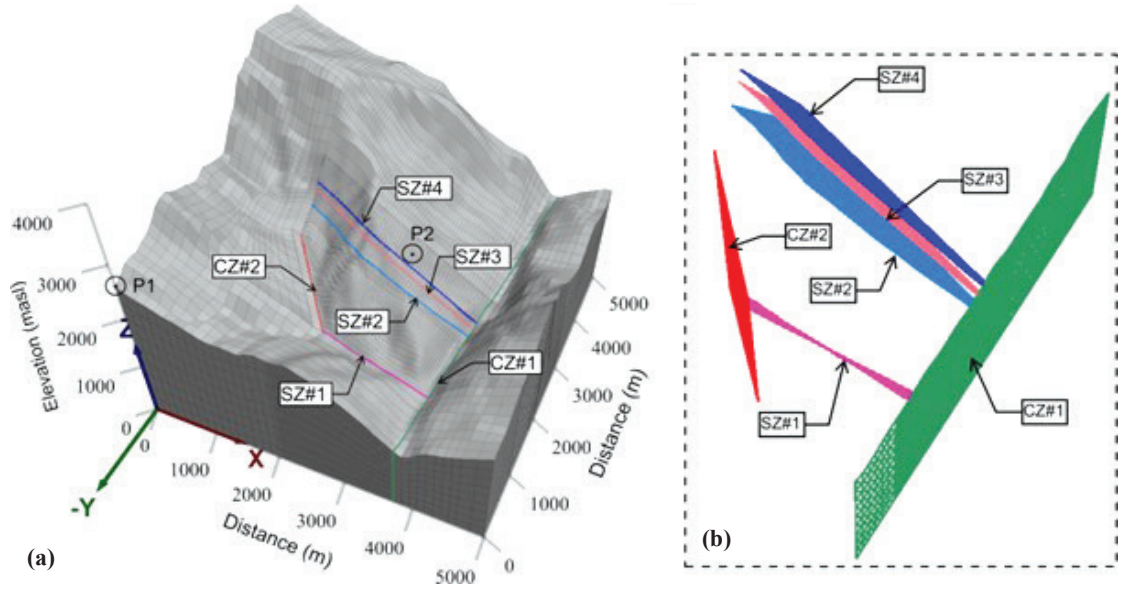

Fig. 7: 3D geometry with (a) actual topographic condition, (b) weakness and shear zones.

Input parameters

The input parameters required for the model were quantified based on the detail mapping, information received from Tamakoshi project and laboratory testing. The rock mass parameters, interface parameters and tectonic stresses are the most important input variables to be quantified in carrying out numerical analysis. Table 3 shows mean values of rock mass parameters consisting uniaxial compressive strength of intact rock (σ_{ci}), Young's modulus of intact rock (E_i), Poisson's ratio (ν) and unit weight of the rock (γ_r) and their respective standard deviation. The bulk modulus (K) and shear modulus (G) of the intact rock in Table 4 were calculated following the equations suggested by Goodman (1989) for isotropic rock material.

The interface parameters such as stiffness and friction angle are important parameters to the numerical simulation using FLAC^{3D}. Rock mass stiffness of the weakness and shear zones depends on the elasticity modulus (E_0) and shear modulus (G_0) and the thickness of the zone itself. Figure 8 shows both normal stress (S_n) and shear stress (S_s) acting on the weakness. The normal stiffness (k_n) and shear stiffness (k_s) of the weakness and shear zones were estimated using the equations shown within Figure 8 using the values E_0, G_0 and thickness of the zone (t).

Table 3: Mechanical properties of schistose gneiss and input parameters to FLAC^{3D}.

Parameters	Unit	Statistical values	
		Mean	Sd
Density, γ_r	kg/m^3	2745	26
Poisson's ratio, ν		0.2	0.1
Intact rock strength (UCS), σ_{ci}	MPa	61	18
Young's modulus, E_i	GPa	30.2	7.9
Bulk modulus, K	GPa	16.8	5.5
Shear modulus, G	GPa	12.6	4.0

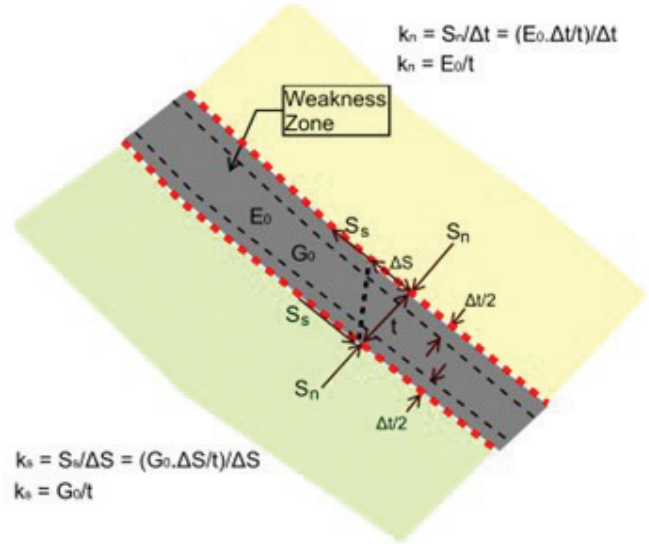

Fig. 8: Weakness zone in between the relatively stiff rock masses.

The elasticity modulus (E_0) of the material of weakness zones was assumed equal to the deformation modulus of the rock mass as recommended by Hoek et al. (1998). Hoek and Diederichs (2006) relationship was used to calculate the deformation modulus of the weakness zone material. Average Q-value (Barton et al., 1974) of most of the weakness and shear zones mapped along the headrace and tailrace tunnels was approximately 0.05, which gives GSI value of approximately 25. The estimated and calculated interface parameters are shown in Table 4 where ν_0 is the Poisson's ratio of the weakness zone rock material, which is taken as 0.1 based on Panthi (2006).

Friction angle of the interface is also an important parameter to be estimated for the simulation. In general, it ranges from 15 to 30° in case of faults and weakness zones (Barton, 1973). Friction angle of 25° was estimated as the most likely value

based on the observation and rock mass quality description of the weakness and shear zones met at the tailrace and headrace tunnels.

Seismic acceleration at the model base

The peak ground acceleration (PGA) values represent the worst-case scenario that give maximum change in the in-situ stress magnitudes. The seismic acceleration at the base was considered having sinusoidal wave. The base acceleration (a_{base}) at time t can then be expressed by Equation 1 (ITASCA, 2017).

$$a_{base} = E_f \times A_{base} \sin(2\pi f t) \qquad (1)$$

$$E_f = \frac{1}{2}\left(1 - \cos\left(\frac{2\pi}{T}t\right)\right) \qquad (2)$$

where, T is the total duration of the wave, f is the frequency of the wave and A_{base} is the amplitude of the wave and E_f is an envelope function (Eq. 2). The envelope function provides a gradual built-up and decay of the wave over the total duration of the wave. The base acceleration was considered as that recorded in the seismic stations at Kathmandu for the aftershock of M_W 7.3. According to Bhattarai et al. (2015) the corresponding frequency of seismic wave was about 1 Hz.

RESULTS AND DISCUSSIONS

The simulation results have indicated that there is a significant influence by tectonic stress on the overall stress state of Tamakoshi area. The model was validated for maximum tectonic stress of 20 MPa with an orientation of N25°E at the base of the model. The corresponding minimum tectonic stress was about 5 MPa. After validation, the magnitude of minimum principal stress was extracted from the model for further assessment on the applicability of shotcrete lined pressure tunnel. The magnitudes of minimum principal stress at the vertical sections cut along both OLD HRT alignment and NEW HRT alignment are shown respectively in Figure 9a,b. The stress trajectories are attenuated due to the presence of different shear zones (Fig. 9).

The magnitudes of minimum principal stresses were extracted from the model results of both static and dynamic analysis so that an overview of their magnitude is statistically assessed with respect to the static water head (P_w) acting along the tunnel alignment. Both minimum principal stress magnitudes and water pressure were plotted for both OLD HRT (Fig. 10a) and NEW HRT (Fig. 10b) alignments. Minimum principal stress magnitudes are considerably lower than that of the static water pressure acting at the headrace tunnel, which indicates that there was high risk of hydraulic jacking (Fig. 10). In addition, one can see that at each dynamic (seismic) loading, there was risk of reduction in the minimum principal stress magnitudes at the areas where shear zones are located.

In addition, the ground shaking due to earthquake had considerable impact on the rock mass located at the high relief area with lower lateral confinement due to steep topography at the outer reach of the headrace tunnel (Fig. 10). However, it is noted here that the minimum principal stress magnitudes at locations upstream from SZ#2 at OLD HRT and form SZ#4 at NEW HRT alignments are not affected by the dynamic loading. This indicates that if the rock mass is strong, homogeneous and of good quality, the risk of de-stressing effect is minimum and in fact the stresses may be accumulated due to such dynamic loading.

Likewise, an assessment was carried out to check the pattern of changes in the magnitude of minimum principal stresses during the shaking period of 60 Sec at selected locations representing

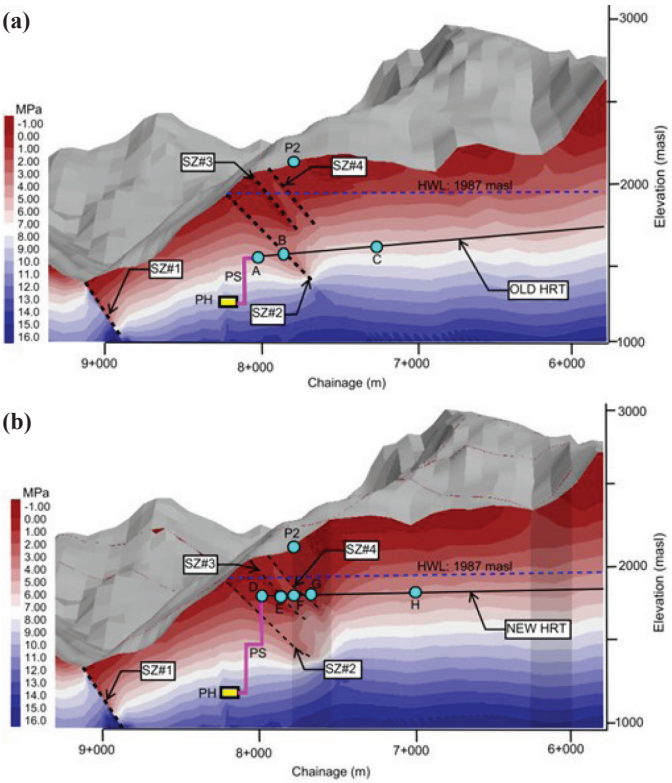

Fig. 9: Minimum principal stress in MPa after static analysis (a) along Old HRT (Y-Y) alignment, (b) along NEW HRT alignment.

Table 4: Input parameters for interfaces.

Interfaces	E_i GPa	Q	GSI	E_0 GPa	ν_0	G_0 GPa	t m	k_n Pa/m	k_s Pa/m	Friction angle (°)
CZ#1	30.2	0.05	25	1.8	0.1	0.82	35	5.1E+07	2.3E+07	25
CZ#2	30.2	0.05	25	1.8	0.1	0.82	25	7.2E+07	3.3E+07	25
SZ#1	30.2	0.05	25	1.8	0.1	0.82	25	7.2E+07	3.3E+07	25
SZ#2	30.2	0.05	25	1.8	0.1	0.82	30	6.0E+07	2.7E+07	25
SZ#3	30.2	0.05	25	1.8	0.1	0.82	35	5.1E+07	2.3E+07	25
SZ#4	30.2	0.05	25	1.8	0.1	0.82	15	1.2E+08	5.5E+07	25

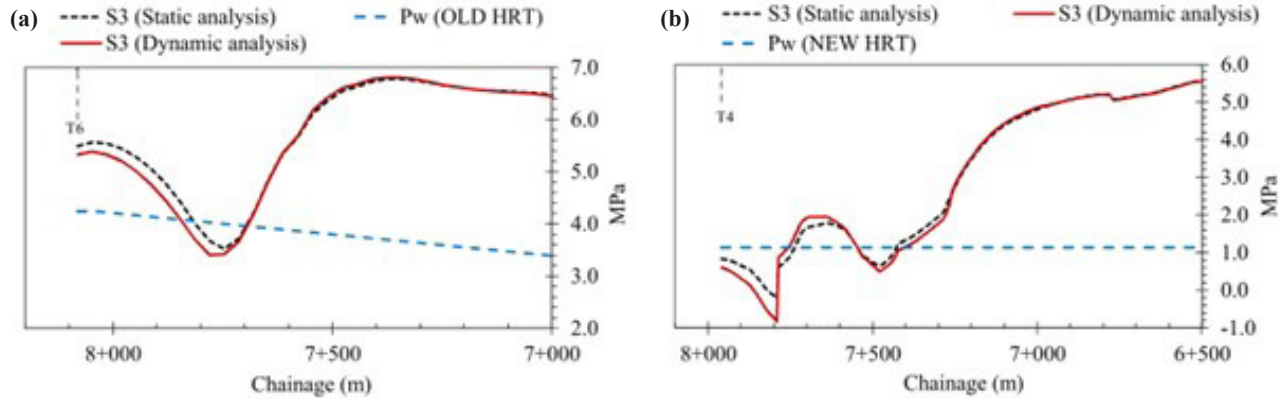

Fig. 10: Minimum principal stresses for both static and dynamic conditions and static water pressure (Pw) along the headrace tunnel (a) Old HRT, (b) New HRT alignments.

A, B, C, D, E, F, G and H marked in Figure 9. It was observed that there is considerable fluctuation in the stress magnitude during the peak of acceleration and it stabilizes once the peak acceleration dies out. The minimum principal stress magnitude at locations C and H dampened and reached to its original value. These two points are in good quality rock mass and are far from the shear zones. On the other hand, at location B, E and G where shear zones are located, the magnitude of minimum principal stresses were stabilized to a new stress magnitude, which was found to be much lower than that of the original one. This indicates that the weakness and fault zones are vulnerable areas during seismic events and permanent change in the in-situ stress state are eminent.

CONCLUSIONS

The static simulation carried out to assess the magnitude of in-situ minimum principal stress suggests that the stress state at the outer reach of shotcrete lined headrace tunnel at Upper Tamakoshi Hydroelectric Project is very much influenced by the slope topography of two valleys and the presence of weakness and shear zones. The dynamic seismic simulation further indicated that a permanent reduction in the in-situ stress state occurs in areas where weakness and shear zones are located. This suggests that the dynamic loading caused by large scale earthquakes may further increase the risk of hydraulic jacking and potential leakage through the weakness zones areas if these are not fully lined.

REFERENCES

Basnet, C. B. and Panthi, K. K., 2021, Evaluation of in situ stress state along the shotcrete lined high-pressure headrace tunnel at a complex Himalayan geological condition. Geosystem Engineering, v. 24(1), pp. 1–17.

Barton, N., 1973, A review of the shear strength of filled discontinuities in rock. Fjellspregningsteknikk, Bergmekanikk, Oslo. Tapir Press, Trondheim, pp. 19.1–19.38.

Barton, N., Lien, R., and Lunde, J., 1974, Engineering classification of rock masses for the design of tunnel support. Rock Mechanics, v. 6, pp. 189–236.

Bhattarai, M., Adhikari, L. B., Gautam, U. P., Laurendeau, A., Labonne, C., Hoste-Colomer, R., Sebe, O., and Hernandez, B., 2015, Overview of the large 25 April 2015 Gorkha Nepal earthquake from accelerometric perspectives. Seismological Research Letters, v. 86(6), pp. 1540–1548.

Goodman, R. E., 1989, *Introduction to rock mechanics*, 2nd Edition, Wiley, New York, 576 p.

Hoek, E., Marinos, P., and Benissi, M., 1998, Applicability of the Geological Strength Index (GSI) classification for very weak and sheared rock masses. The case of the Athens Schist Formation. Bulletin of Engineering Geology and the Environment, v. 57(2), pp. 151–160.

Hoek, E. and Diederichs, M., 2006, Empirical estimation of rock mass modulus. International Journal of Rock Mechanics and Mining Sciences, v. 43(2), pp. 203–215.

ISRM, 1978, Suggested method for determining indirect tensile strength by the Brazil test. International Journal of Rock Mechanics and Mining Sciences & Geomechanics Abstracts, v. 15(2), pp. 102–103.

ITASCA. 2017. FLAC3D 6.0 User's Manual.

McGarr, A. and Gay, N. C., 1978, State of stress in the Earth's crust. Annual Review of Earth and Planetary Sciences, v. 6(1), pp. 405–436.

Norconsult and Lahmeyer, 2008, Detailed design report of Upper Tamakoshi Hydroelectric Project, Nepal. Nepal Electricity Authority.

Panthi, K. K., 2006, Analysis of engineering geological uncertainties related to tunnelling in Himalayan rock mass conditions. Doctoral theses at NTNU 2006:41. Norwegian University of Science and Technology (NTNU), Norway.

Panthi, K., 2012, Evaluation of rock bursting phenomena in a tunnel in the Himalayas. Bulletin of Engineering Geology and the Environment, v. 71(4), pp. 761–769.

Panthi, K. K., 2014, Norwegian Design Principle for High Pressure Tunnels and Shafts: It's Applicability in the Himalaya. Hydro Nepal: Journal of Water, Energy and Environment, v. 14, pp. 36–40.

Panthi, K. K. and Basnet, C. B., 2017, Design review of the headrace system for the Upper Tamakoshi project, Nepal. The International Journal on Hydropower and Dams, v. 24(1), pp. 60–67.

Panthi, K. K. and Basnet, C. B., 2019, Evaluation of earthquake impact on magnitude of the minimum principal stress along a shotcrete lined pressure tunnel in Nepal. Journal of Rock Mechanics and Geotechnical Engineering, v. 11, pp. 920–934.

SINTEF, 2008, Rock stress measurement at the Upper Tamakoshi Hydroelectric project. SBF IN F08112.

SINTEF, 2013, Rock stress measurement by hydraulic fracturing at the Upper Tamakoshi Hydroelectric project, Nepal. SBF IN F08112.

Stephansson, O. and Zang, A., 2012, ISRM suggested methods for rock stress estimation - part 5: establishing a model for the in-situ stress at a given site. ISRM Suggested Methods for Rock Characterization, Testing and Monitoring: 2007-2014, pp. 187–201.

USGS, 2015, U.S. Geological Survey: ShakeMap of M 7.3 aftershock – 19 km SE of Kodari, Nepal. https://earthquake.usgs.gov/earthquakes/eventpage/us20002ejl#shakemap.